NRL Report 6639

Electron Impact Studies of Volatile Inorganic Compounds

F. E. Saalfeld and M. V. McDowell

Physical Chemistry Branch
Chemistry Division

November 22, 1967

NAVAL RESEARCH LABORATORY
Washington, D.C.

This document has been approved for public release and sale; its distribution is unlimited.

CONTENTS

Abstract ii
Problem Status ii
Authorization ii

INTRODUCTION 1

DEFINITIONS 1

METHODS OF ESTIMATION OF APPEARANCE POTENTIALS FROM IONIZATION-EFFICIENCY CURVES 2

THERMOCHEMICAL RELATIONSHIPS 7

EXPERIMENTAL APPARATUS AND PROCEDURE 9

- Mass Spectrometers 9
- Materials 10

RESULTS AND DISCUSSION 10

- Silylphosphine (H_3SiPH_2) 10
- Silylgermane (H_3SiGeH_3) 13
- Silylarsine (H_3SiAsH_2) 15
- Phosphorus Trifluoride (PF_3), Phosphorus Oxytrifluoride (POF_3), and Phosphorus Pentafluoride (PF_5) 17
- Hydridotrifluorophosphorustricarbonylcobalt [$HCo(CO)_3PF_3$], Hydridobis(trifluorophosphorus)dicarbonylcobalt [$HCo(CO)_2(PF_3)_2$], and Hydridotris(trifluorophosphorus)carbonylcobalt [$HCoCO(PF_3)_3$] 17

CONCLUSIONS 22

ACKNOWLEDGMENTS 22

REFERENCES 24

ABSTRACT

The appearance potential of an ion is defined as the minimum energy of bombarding electrons required to produce that ion from a particular atom or molecule. This potential can be estimated from ionization-efficiency curves by various methods, such as the initial break method, linear extrapolation method, critical slope method, extrapolated difference method, second derivative method, ratio extrapolation method, and energy compensation method.

By the use of appearance-potential data obtained from the mass spectrometer, the bond energies and heats of formation of unstable inorganic materials can be determined. Although there are several possible sources of error in a mass spectrometric thermochemical determination, it is often the only method by which these important properties can be determined for many of the transient and highly reactive molecules and radicals.

Where literature values were available, there was usually good agreement between the thermochemical values determined by mass spectrometric measurement and those found by other methods.

PROBLEM STATUS

This is an interim report; work is continuing on all phases of the problem.

AUTHORIZATION

NRL Problem C07-02
Project RR 001-01-43-4804

Manuscript submitted August 30, 1967.

ELECTRON IMPACT STUDIES OF VOLATILE INORGANIC COMPOUNDS

INTRODUCTION

Mass spectrometers have found practical usage in analytical determinations. The Navy applications of this sophisticated instrument are extremely broad; for example, it has been used to determine the impurities in aviators' oxygen supply (1), to identify the contaminants in spacecraft and nuclear submarine atmospheres (2), to measure the permeability of gases through elastomers (3), and to measure the diffusion of methyl chloroform through insulation materials used in nuclear submarines (4). These examples represent only a few of the applications of mass spectrometers to Navy problems; other studies have been undertaken at NRL to provide the basic information required for the development of other practical applications. This information, dealing primarily with the ionization and dissociation of inorganic molecules under electron impact, can be applied in a number of fields of chemistry and physics, such as gaseous electrical discharges, radiation chemistry, ionic chemical reactions, and thermodynamics.

In a mass spectrometer the gaseous molecules of the sample are usually bombarded by low-, controlled-energy electrons which have been emitted from a heated filament. The electron bombardment ionizes a portion of the gaseous molecules in the ion source of the mass spectrometer; the nonionized sample molecules are removed by evacuation. The ions are accelerated and collimated into a beam by a series of electrode slits, maintained at different electrical potentials, and then the ion beam is mass-analyzed by some method, such as radio frequency, time-of-flight, or magnetic deflection. It is beyond the scope of this report to cover these methods of mass analysis, which are adequately described by Beynon (5); it is sufficient to say here that each method of mass separation has some advantages and disadvantages.

After the ion beam has been mass-analyzed, the separated ions having the same mass-to-charge ratio (m/e) pass through a slit and impinge on a collector. The electrical signal generated from the ion beam is amplified by an electron multiplier, vacuum-tube-electrometer amplifier, a vibrating-reed electrometer, or some other method, and the resulting voltage recorded.

DEFINITIONS

The mass spectrum of a molecule consists of series of m/e-ion-current intensities, resulting from the degradation of the molecule after electron impact. This *fragmentation pattern* is a characteristic of the molecule which is dependent on the electron energy. There are two main ways to present the fragmentation-pattern data. The most widely used approach is to give the ion-current intensities relative to the largest m/e-ion current (called the "base peak") which is taken as 100. In the second method the individual m/e intensities are cited as percent of the total ion current of the entire spectrum. The various types of ions which may be observed in the mass spectrum are the parent ion, molecule ions, fragment ions, doubly charged ions, metastable ions and rearrangement ions (all of the preceding have a positive charge), and negative ions. *Parent ions* are a result of the molecules under study losing one electron. *Molecule ions,* frequently confused with parent ions, are ion molecules which are eliminated from the original molecule; e.g., with the molecule C_4H_9OH the parent ion $C_4H_9OH^+$ eliminates H_2O^+ which is a

molecule ion. *Fragment ions* are produced from the parent ion by rupture of one or more bonds. *Doubly charged ions* are those ions resulting from the removal of two electrons; *metastable ions* are those ions which are accelerated at one mass, then decompose to an ion of lower m/e and a neutral radical or molecules and are mass-analyzed at the second m/e. The *rearrangement ions* are a result of the alteration of the molecular orientation of the original molecule by electron impact; e.g., ion $A\text{-}B\text{-}C\text{-}D^+$ produces the fragment ion $A\text{-}D^+$ in a rearrangement process. Finally, *negative ions* are formed in the spectrum by either electron capture or ion-pair formation.

The *appearance potential* of an ion is defined as the minimum energy of the bombarding electrons required to produce that ion *from a particular atom or molecule*. If the electrical potential between the ion source of the mass spectrometer and the filament which emits the bombarding electrons is reduced by some means, the energy of the electrons passing through the ion source consequently is lowered. As this electron energy is reduced, the number of ions produced by electron bombardment also diminishes until finally no ions are produced. The electron energy at which an ion is no longer produced by electron impact depends on several parameters, such as the ionization potential of the molecule, the number of bonds broken to form the fragment ion from the parent ion, and, indeed, the general nature of the molecule under investigation. A graphical representation of the variation of an ion-current intensity (peak height) as a function of the energy of the ionizing electrons is known as the *ionization-efficiency curve*. A typical curve, shown in Fig. 1, when measured on conventional mass spectrometers, generally consists of four sections: (a) a curved portion for the first volt or so above the appearance potential, (b) a linear increase for the next 10 to 20 v, (c) a broad plateau-shaped maximum between 50 and 100 v, and (d) a gradual decrease in intensity on further increase in the ionization energy. Not all ionization-efficiency curves have exactly the same shape; for example, ions which are most abundant in the mass spectrum tend to have a shorter initial curved portion and longer linear region of their ionization-efficiency curves than ions which are less abundant (Fig. 2).

The method of measuring appearance potentials is simple in principle. The accelerating voltage, or magnetic field, of the mass spectrometer is adjusted so that the desired m/e species passes through the analyzer and is focused on the collector. The energy of the bombarding electrons is then reduced, and the decreasing ion current continuously recorded. The voltage measured at the minimum energy, however, does not represent the exact appearance potential of the m/e species in question but differs from the true value by a contact-potential difference and usually some thermal energies. The contact potentials are normally corrected by comparing the measured appearance potential of the m/e ion of interest to the measured appearance potential of a rare gas, such as argon or krypton, whose ionization potential (the appearance potential of a parent ion) is accurately known from optical spectroscopy data. It is particularly important that the sample and the rare gas (known as the internal standard) are introduced into the mass spectrometer concurrently, because the contact potential depends not only on the metal used in the ion source but also on the nature and amount of contamination of the source surfaces. Since the surface contamination may change considerably (as much as 1 v or more) when the sample is introduced, both the calibrating gas and the sample must be studied under identical conditions. Many sources of error can enter into appearance-potential measurements, but most of these lie outside the scope of this report and have been thoroughly discussed by Waldron and Wood (6).

METHODS OF ESTIMATION OF APPEARANCE POTENTIALS FROM IONIZATION-EFFICIENCY CURVES

Because many experimental and theoretical factors influence the ionization-efficiency curve, there has been extensive debate as to how the appearance potential should be estimated from the ionization-efficiency curve. A critical evaluation of the various methods

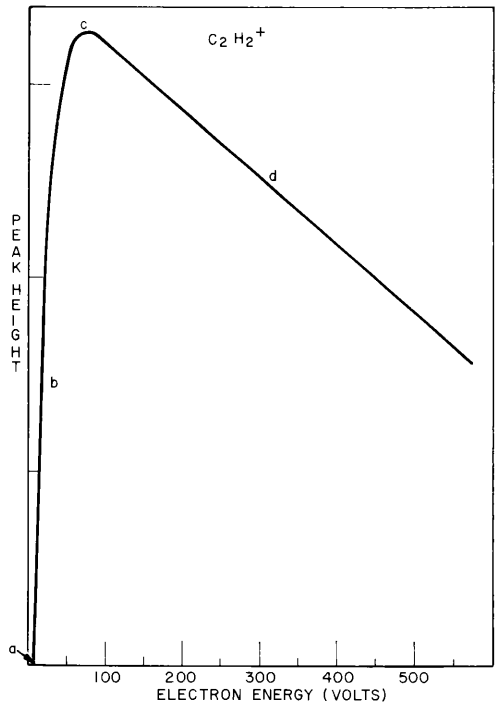

Fig. 1 - Ionization-efficiency curve for acetylene - a typical ionization-efficiency curve

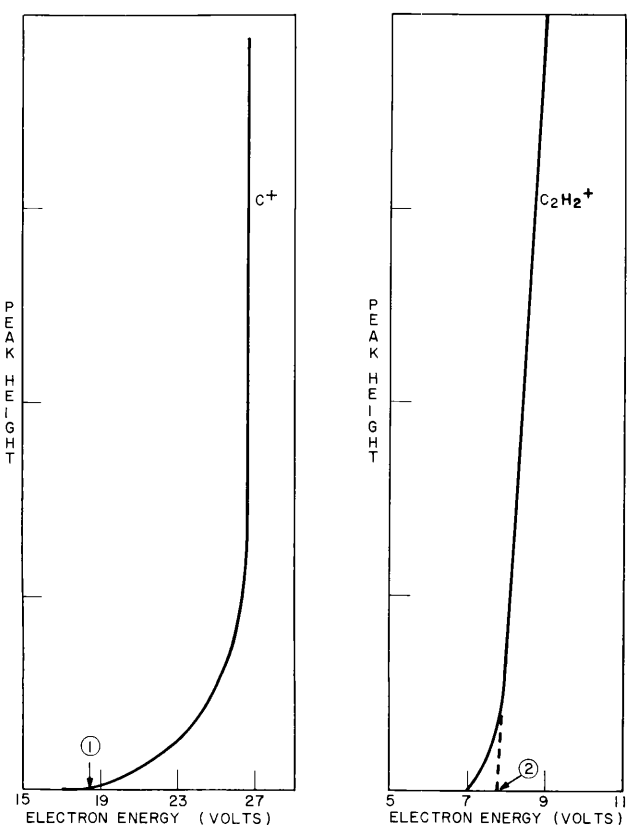

Fig. 2 - Ionization-efficiency curves for high-intensity ($C_2H_2^+$; 100) and low-intensity (C^+; 2.5) ions from acetylene (internal standard ionization-efficiency curves are not shown)

is outside the scope of this report; however, each of the methods has some theoretical or experimental drawback. These points are covered in detail by Field and Franklin (7).

The *initial break method* (also known as the *vanishing current method*) takes as the appearance potential the electron voltage corresponding to the first formation of the ion of interest (point 1 in Fig. 2). This method is influenced by such factors as the pressure of the gas being investigated and the sensitivity of the amplifier.

A second method of appearance-potential estimation is the *linear extrapolation method*. In this method the rising linear portion of the ionization-efficiency curve is extrapolated to zero ion current (point 2 in Fig. 2). It is obvious that for this method to be usable the ionization-efficiency curves of both the sample and calibrating gas must have a linear portion and similar shapes.

The *critical slope method* of determining appearance potentials uses a semilog plot of an ionization-efficiency curve; the point (C in Fig. 3) on this curve which has a slope of (2/3)/(kT) is taken as the onset potential. T is the absolute temperature of the mass spectrometer filament, and k is the Boltzmann constant. This method has not been used for determining the appearance potential of fragment ions but gives excellent results for the ionization potentials of molecular ions.

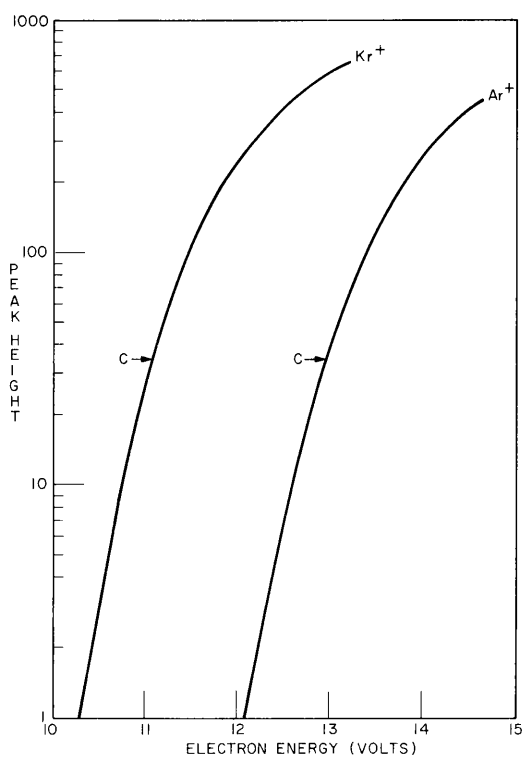

Fig. 3 - Semilog plot of ionization-efficiency curve; C denotes the calculated critical isotope which is taken as the appearance potential

The *extrapolated difference method* shown in Fig. 4 is one of the two methods used by the author to evaluate appearance-potential data. In this method the ionization-efficiency curves for the sample and reference gases are plotted with the ordinate scales chosen so as to make the linear portions of the two curves essentially parallel. The differences of the electron voltage ΔV between the curve for the sample and the reference gas corresponding to various values of the ion current I are then replotted and extrapolated to zero ion current. The extrapolated value of ΔV is taken as the difference between the two appearance potentials. This method is a modification of the initial break method and is not suited for ions of very low intensity.

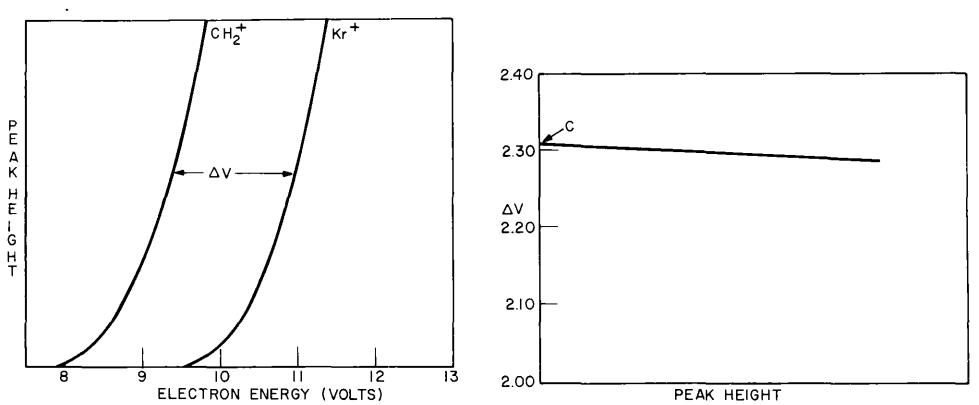

Fig. 4 - The extrapolated difference method of appearance-potential measurements; the arrow indicates the difference between the appearance potential of Kr and the CH_2 radical

In the *semilog* plots of the ionization curves, shown in Fig. 5, the threshold potential is taken as the electron energy at which the ion current is 1% of its value when the electron energy is 50 v. Again, the method works best with molecular ions and other ions where the calibrating-gas and sample ionization-efficiency curves have similar shapes. Morrison and his coworkers have employed a method (7), shown in Fig. 6, which uses the *second derivative* of the ionization-efficiency curve to determine appearance potentials. This method works well with simple molecules but has not been adequately tested for complex or low abundance ions.

Two other methods of appearance-potential assessment have been proposed recently for use with low intensity fragment ions and ions formed from reactive molecules. Svec and his coworkers (8) use the *ratio extrapolation method*, where the ion currents of both the sample and the calibrating gas are recorded alternately at two electron energies, one a reference voltage and the other a variable voltage. The second derivative of the ratio of the ion currents observed at the variable energy to that observed at the constant energy is plotted against the numerical value of decreasing electron energy and the resulting linear portion of the ionization-efficiency curve extrapolated to zero. This method is the second method used by the author to obtain appearance-potential values and is illustrated in Fig. 7.

Kiser and his students have developed their *energy compensation method* (9), where the ion currents for the sample and internal standard are recorded at 50 v, the sensitivity of the amplifier then increased 100 or 1000 times, and the electron energy reduced until an ion-current reading equal to the value of the 50-v reading is observed. The value of the electron energy at this second ion-current value (at the increased amplifier position)

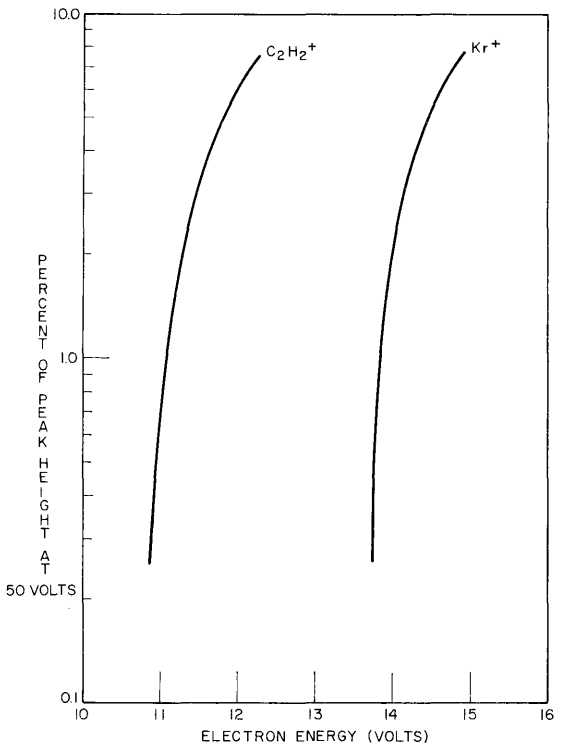

Fig. 5 - Semilog method of evaluating the appearance potential of acetylene

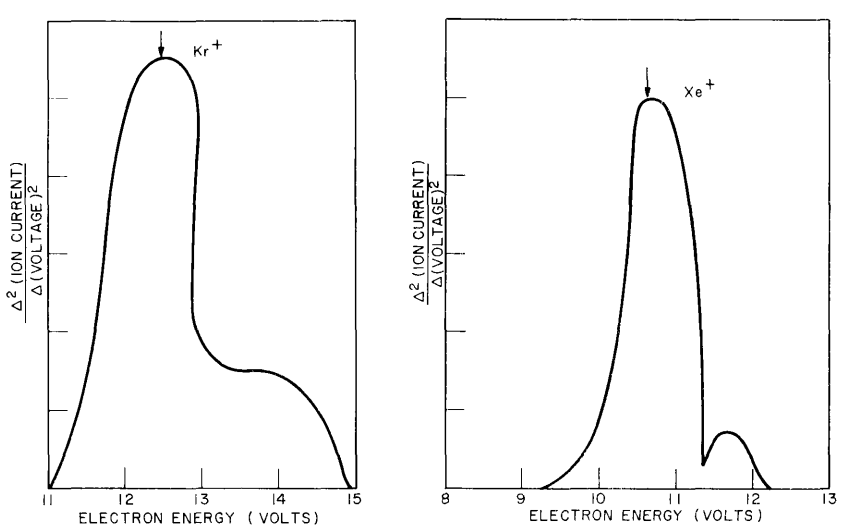

Fig. 6 - Second derivative ionization-efficiency (the arrow on each curve denotes the appearance potential)

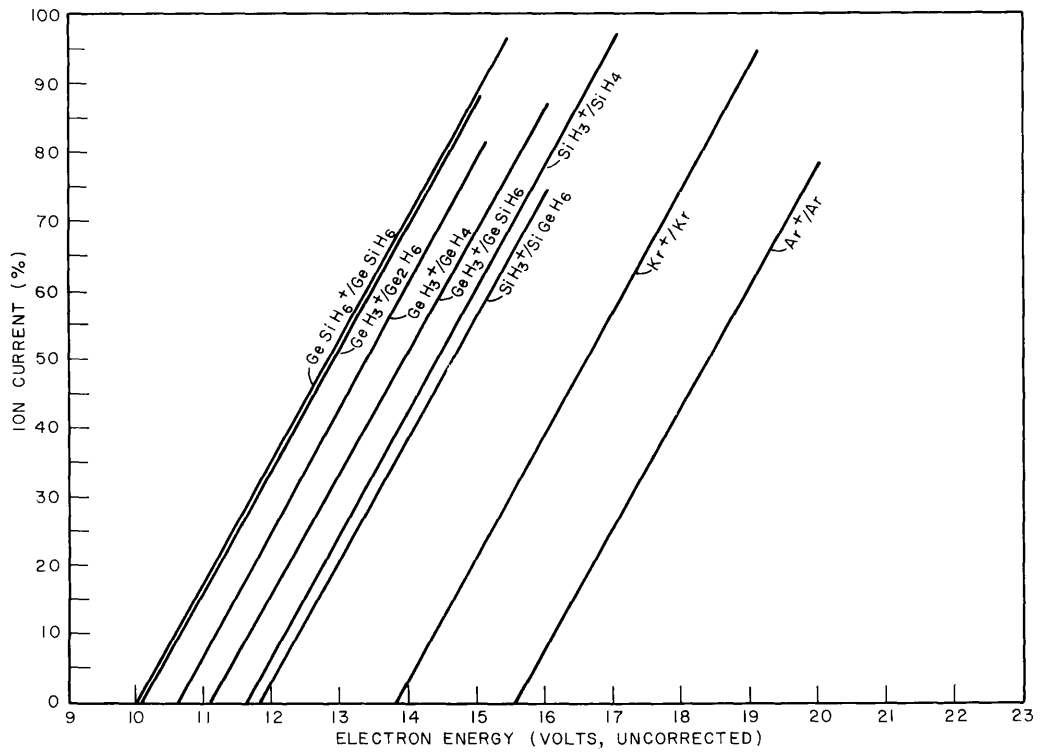

Fig. 7 - Ratio-extrapolation method of estimating the appearance potential; ionization-efficiency curves for selected ions from $GeSiH_6$, Si_2H_6, GeH_6, SiH_4, and GeH_4

is taken as the appearance potential. This method is a simplified version of the semilog method.

THERMOCHEMICAL RELATIONSHIPS

Thermochemical quantities can be derived from appearance-potential (ap) measurements since these quantities correspond directly to ΔE for the reaction occurring in the ion source. However, for such an ion-source reaction the magnitude of $\Delta(PV)$ is negligible so

$$ap = \Delta E = \Delta H - \Delta(PV) \cong \Delta H_{reaction} .$$

If a reasonable ion-source reaction can be assumed, heats of formation ΔH_f° and bond-dissociation energies DE can be calculated from appearance-potential data. For example, from an ion-source reaction, such as

$$R_1R_2 + e^- \rightarrow R_1^+ + \cdot R_2 + 2e^- \tag{1}$$

and Hess's law of elementary thermodynamics

$$\Delta H^\circ_{reaction} = \Sigma(\Delta H^\circ_{f\ products}) - \Sigma(\Delta H^\circ_{f\ reactants}),$$

we have

$$ap\ (R_1^+) = \Delta H^\circ_{reaction} = \Delta H^\circ_f(R_1^+) + \Delta H^\circ_f(\cdot R_2) - \Delta H^\circ_f(R_1R_2) + KE + EE\ , \quad (2)$$

where KE is the kinetic energy of the particles produced in the ion-source reaction and EE is their excitation energy (electronic, vibrational, and rotational). Bond-dissociation energies and the radical ionization potential are related to the appearance potential by the equation

$$ap\ (R_1^+) = I(R_1) + DE(R_1 - R_2) + KE + EE\ , \quad (3)$$

where $I(R_1)$ is the ionization potential of the radical R_1, DE is the bond dissociation energy of $R_1 - R_2$, and KE and EE are the excess energies mentioned above. In general, EE is quite small and usually neglected. KE is difficult to measure, and although the particles formed in the ion-source reaction may or may not contain appreciable kinetic energy, it is normally assumed that this energy is either absent or negligible. Thus, Eqs. (2) and (3) become

$$ap\ (R_1^+) \geqq \Delta H^\circ_f(R_1^+) + \Delta H^\circ_f(R_2) - \Delta H^\circ_f(R_1R_2) \quad (4)$$

and

$$ap\ (R_1^+) \geqq I(R_1) + DE(R_1 - R_2)\ , \quad (5)$$

according to whether or not KE and EE can be neglected. It can be seen that when $\Delta H^\circ_f(R_1R_2)$ is determined from appearance-potential data, where KE and EE have been *assumed* to be zero or negligible, the value obtained must be considered a *lower limit* of the true value. Similarly, if Eq. (5) is used with appearance-potential data to estimate the bond energy $DE(R_1 - R_2)$, the value cited should be taken as an *upper limit* to the actual bond energy.

One additional caution in using appearance-potential data to calculate ΔH°_f and DE should be pointed out; i.e., one never knows with absolute assurance the ion-source reaction. This situation occurs because the neutral species of the reaction cannot be readily observed in the mass spectrometer. With some diatomic molecules the neutral species can be assumed with an extremely high degree of certainty (e.g., in the ion-source reaction $H_2 + e \rightarrow H^+ + H + 2e$, there is little doubt as to the nature of the neutral fragment), but with polyatomic molecules the choice is not always as clearcut (e.g., in the ion-source reaction $CH_4 + e^- \rightarrow CH_2^+$ + neutral product(s), is the hydrogen present as a H_2 molecule or two $\cdot H$ atoms?). Several methods are available for making educated estimates, such as the presence of metastable ions, which, if present, indicate a certain ion-source reaction but, by itself, does not give the exact nature of the neutral product. However, the absence of a specific metastable peak does not rule out an ion-source reaction. Beynon (5) has thoroughly discussed the use of metastable ions in his book. Another source of ion-source-reaction information is the clastogram. This concept, originated by Kiser (10), uses a plot of the fragmentation pattern of a molecule versus the electron energies and, under favorable circumstances, depicts the growth of one specie at the expense of another as the electron energy is varied and gives a clue to the identity of the neutral product. Finally, the heats of formation of the ions obtained from the appearance-potential measurements must be reasonable and the shape of the ionization-efficiency curve studied for clues to the identity of the neutral product.

To sum up, the weakest points in using appearance-potential data to calculate ΔH°_f and DE are: (a) there is no theoretically sound method to interpret *all* ionization-efficiency curves; (b) KE and EE are normally assumed to be either zero or negligible, but there is no readily usable method of testing these assumptions; and (c) the ion-source reactions assume the nature of the neutral species. Despite the drawbacks, the use of appearance-potential data is sometimes the only means available to estimate the important thermochemical properties ΔH°_f and DE for reactive compounds, radicals, and compounds which can be made in only minute quantities (e.g., micrograms or less).

One, however, should always bear in mind the assumptions and limitations of the appearance-potential method of obtaining thermochemical data.

EXPERIMENTAL APPARATUS AND PROCEDURE

Mass Spectrometers

Two mass spectrometers have been employed in these studies. The first spectrometer is a Consolidated Electrodynamic Corp. (CEC) 21-103C, which has been modified at NRL for appearance-potential studies. This instrument is a magnetic-deflection type, where the ion beam is bent 180 degrees. An Applied Physics Corp. Model 36 vibrating-reed electrometer was used to amplify the ion currents. The following conditions prevailed in the ion source during the measurements: the ionizing current was 10.5 μamp, the repeller potentials were adjusted to give maximum-intensity flat-topped peaks for the fragmentation patterns and were shorted together and held at 2.5 v positive with respect to the ion-source chamber for the appearance-potential studies, the ion-source temperature was 250°C, and the instrument was operated in the focused mode. The electron energy was varied by 0.1-v increments for appearance-potential measurements, and the ion accelerating potential was maintained at 2000 v, with the magnetic field being manually adjusted to bring the desired m/e to focus on the ion collector. The fragmentation patterns were measured by continuously decreasing the ion accelerating voltage with a constant magnetic field and an electron energy of 70 v. The ratio extrapolation method of Svec was normally employed to interpret the appearance-potential data obtained on this mass spectrometer. The results obtained by this method of interpretation agreed, within the experimental error, with other methods, such as semilog plots and extrapolated differences. The ratio-extrapolation method was preferred because of its simplicity and the way in which it emphasizes different ion-source reactions.

The second mass spectrometer used in these studies was an NRL-modified Bendix Time-of-Flight (T-O-F) instrument, which was operated in the pulsed-ion mode. The NRL modification (11), which takes advantage of the multiple-analog output system of the Bendix instrument, permits the chart drive of a two-pen recorder to be synchronized with the continuously decreasing voltage of the electron-energy control. The electron-energy-control potentiometer is rotated by a synchronous 60-cps motor, mechanically coupled to the potentiometer drive shaft through a gear rack. A start-stop timer energizes simultaneously the chart drive and the electron-energy-control drive motor. It was possible to obtain the ionization-efficiency curves for two ions (an ion from the sample and the internal standard used to calibrate the voltage scale) simultaneously in less than one minute with this modification. The fragmentation patterns were obtained using electrons having 70 v of energy and an ionizing current controlled at 0.125 μamp. The appearance potentials were estimated from the Bendix data by the extrapolated-difference method.

Several factors dictated which mass spectrometer was to be used. The ion source in the Bendix mass spectrometer is not heated, and the appearance-potential data could be obtained much faster on this instrument than on the Consolidated mass spectrometer. Thus, when the compound being studied was either thermally unstable or could be prepared in only minute amounts, the Bendix mass spectrometer was preferred; whereas, when a large amount of sample was available, the CEC 21-103c, with its more reproducible fragmentation-pattern data, was employed. Another factor in favor of the Bendix instrument is that the ionization-efficiency curve for both the ion of interest and the calibrating gas can be measured simultaneously; with the CEC 21-103c, even though the two gases were introduced into the instrument concurrently, first one curve is measured and then the other. It was necessary to assume that no change in the contact potentials or other variable had occurred in the time needed to take the data; this situation can never be exactly the case, because some of the gases are removed by evacuation while the first

measurement is being made. For these reasons the appearance-potential data obtained from the Bendix are considered to be more reliable than those measured on the Consolidated instrument.

Materials

Silylphosphine (H_3SiPH_2) - Silylphosphine was prepared and separated by the method of Drake and Jolly (12) in a vacuum system which contained no grease. Equimolar amounts of silane and phosphine obtained from a commercial source were circulated through a silent electric discharge, operated at 6-kv ac, and a U-trap, cooled with an ethanol slush (-125°C) for 6 hours. At 1-hour intervals the discharge was stopped, the U-trap was cooled with liquid nitrogen, and any volatile substances remaining in the system were quickly removed by evacuation. The compounds formed in the discharge reaction were separated by fractional distillation using conventional vacuum techniques (13).

Silylgermane (H_3SiGeH_3) - Silylgermane was prepared by the procedure of Spanier and MacDiarmid (14) by passing a 1:1 mixture of silane and germane through a silent, electric discharge. The silane and germane were prepared by standard methods (15) from the enriched isotopes ^{28}Si (99.38%) and ^{74}Ge (96.06%). Trap-to-trap distillation was employed to separate the products of the discharge reaction.

Silylarsine (H_3SiAsH_2) - Silylarsine was prepared by the method described above (12) for silylphosphine. Silylarsine and tetrasilane, Si_4H_{10}, were separated from the other compounds formed in the discharge reaction by fractional distillation using conventional vacuum techniques (13). It was not possible to completely separate silylarsine from tetrasilane by either distillation or with a gas-liquid chromatographic column (12 ft by 0.25 in. I.D.), packed with 10% Silicone 702 on Celite.

Phosphorus Trifluoride (PF_3), Phosphorus Pentafluoride (PF_5), and Phosphorus Oxytrifluoride (POF_3) - Phosphorus trifluoride was obtained from a commercial source and used without further purification. However, the phosphorus pentafluoride, also obtained commercially, was contaminated with phosphorus oxytrifluoride; the amount of the phosphorus oxytrifluoride increased with the length of time that the sample was stored in the stainless-steel inlet system of the Bendix T-O-F mass spectrometer. After a 92-hour retention in the inlet system, mass spectrometric analysis showed the gas to be essentially pure phosphorus oxytrifluoride. Thus, the spectra of this compound could be obtained and the spectral properties of phosphorus pentafluoride obtained from the original commercial mixture by difference.

Hydridotrifluorophosphorustricarbonylcobalt [$HCo(CO)_3PF_3$], Hydridobis(trifluorophosphorus)dicarbonylcobalt [$HCo(CO)_2(PF_3)_2$], and Hydridotris(trifluorophosphorus)carbonylcobalt [$HCoCO(PF_3)_3$] - These compounds were prepared and purified by Professor A. G. MacDiarmid and Dr. Surinder K. Gondal of the University of Pennsylvania. They were used without further purification.

RESULTS AND DISCUSSION

Silylphosphine (H_3SiPH_2)

The fragmentation pattern of the positive ions of silylphosphine is shown in Table 1. The pattern was calculated using the following isotope abundances: ^{28}Si - 92.18, ^{29}Si - 4.71, and ^{30}Si - 3.12 (5).

The appearance potentials (ap), postulated ion-source reactions, and thermochemical calculations are given in Table 2. Krypton was used as an internal standard to calibrate

Table 1
Monoisotopic Positive Fragmentation Pattern of Silylphosphine* (70-ev Electrons)

Ion	Percent of Total Ion Current	Ion	Percent of Total Ion Current
$SiPH_5^+$	3.4	PH^+	1.5
$SiPH_4^+$	6.2	P^+	0.6
$SiPH_3^+$	6.0	SiH_3^+	1.0
$SiPH_2^+$	4.1	SiH_2^+	0.6
$SiPH^+$	58.4	SiH^+	0.2
SiP^+	15.2	Si^+	–
PH_2^+	2.9		

*Data obtained on the CEC 21-103c mass spectrometer.

the electron-voltage scale. As an accuracy check, argon was introduced with the krypton and the hydride sample. The ionization potential of argon was then determined with the voltage-scale correction found from the krypton measurement. By this method the maximum possible error in the absolute accuracy was estimated to be ±0.2 v; however, the precision of the measurement was better than ±0.1 v. The electron affinities of $\cdot PH_2$ and $\cdot SiH_3$, presented in Table 2, were calculated by the method of Neale (16). It has been assumed that no excess kinetic energy is contained in the measured appearance potentials. Since this assumption could not be adequately tested in these measurements, the values for appearance potentials presented in Table 2 may be greater than the true ones; however, on the basis of previous work (17,18) this discrepancy is thought to be unlikely. The ancillary values used in the calculations of Table 2 were taken from the data of Gunn and Green (19) and are (in kcal/mole): $\Delta H_f^\circ(H) = 52.1$, $\Delta H_f^\circ(SiH_4) = 7.3$, $\Delta H_f^\circ(Si_2H_6) = 17.1$, $\Delta H_f^\circ(PH_3) = 1.3$, and $\Delta H_f^\circ(P_2H_4) = 5.0$.

There are three notable disagreements between the data presented in Table 2 and previously published values of $IP(\cdot SiH_3)$, $\Delta H_f^\circ(\cdot SiH_3)$, and ap $(\cdot PH_2^+)$ from PH_3. The first two differ from the results cited by Steele, et al. (20). These authors do not mention the ion-source conditions under which their measurements were made. It has been found here that variations in source conditions can drastically affect the values obtained for the appearance potentials of fragment ions. This effect is especially dependent upon the repeller voltage settings. The values presented here are lower than Steele's; so it is possible that his values include some excess kinetic energy. Since both sets of data were obtained with the same type mass spectrometer (CEC 21-103c), this assumption is a reasonable explanation for the discrepancy. In the third case the ap (PH_2^+) from PH_3 did not agree with the value given previously by Saalfeld and Svec (17) but did agree with a recent result by Wada and Kiser (21). Subsequent review of the data obtained by Saalfeld and Svec showed that through an arithmetical mistake a value of 14.4 ev instead of 13.4 was recorded for ap (PH_2^+) from PH_3. Thus, the three measured values for this quantity are in good agreement.

It is interesting to note the trends in the data. As would be expected, considering that $\cdot SiH_3$ and $\cdot PH_2$ have different electronegativities, $DE(H_3Si{-}PH_2)$ is greater than either $DE(H_2P{-}PH_2)$ or $DE(H_3Si{-}SiH_3)$. The ionization potential of $\cdot SiH_3$ is lower than that of $\cdot CH_3$, and $IP(\cdot PH_2)$ is lower than $IP(\cdot NH_2)$, agreeing with the concept that the ionization potential should decrease in a chemical group as the atomic number increases. Similarly, the ionization potential is expected to increase in value as one goes

Table 2
Summary of Thermochemistry of Ion-Source Reactions of Silylphosphine*

Ion-Source Reaction	Appearance Potential		Thermochemical Results	
	Ev	Kcal	Equations	Kcal/mole
$SiH_4 \rightarrow \cdot SiH_3^+ + \cdot H$	11.8	272.0	$\Delta H_f^\circ(\cdot SiH_3^+) = ap - \Delta H_f^\circ(\cdot H) + \Delta H_f^\circ(SiH_4)$	227
			$DE(H_3Si-H) = ap - IP(\cdot SiH_3)$	95
$Si_2H_6 \rightarrow \cdot SiH_3^+ + \cdot SiH_3$	11.3	260.5	$\Delta H_f^\circ(\cdot SiH_3) = ap - \Delta H_f^\circ(\cdot SiH_3^+) + \Delta H_f^\circ(Si_2H_6)$	50
			$IP(\cdot SiH_3) = \Delta H_f^\circ(\cdot SiH_3^+) - \Delta H_f^\circ(\cdot SiH_3)$	177
			$DE(H_3Si-SiH_3) = ap - IP(\cdot SiH_3)$	84
$PH_3 \rightarrow \cdot PH_2^+ + \cdot H$	13.2	304.3	$\Delta H_f^\circ(\cdot PH_2^+) = ap - \Delta H_f^\circ(\cdot H) + \Delta H_f^\circ(PH_3)$	254
			$DE(H_2P-H) = ap - IP(\cdot PH_2)$	90
$P_2H_4 \rightarrow \cdot PH_2^+ + \cdot PH_2$	12.5	288.1	$\Delta H_f^\circ(\cdot PH_2) = ap - \Delta H_f^\circ(\cdot PH_2^+) + \Delta H_f^\circ(P_2H_4)$	40
			$IP(\cdot PH_2) = \Delta H_f^\circ(\cdot PH_2^+) - \Delta H_f^\circ(\cdot PH_2)$	214
			$DE(H_2P-PH_2) = ap - IP(\cdot PH_2)$	74
$SiPH_5 \rightarrow SiPH_5^+$	10.0	230.5	$IP(SiPH_5) = ap$	230
$SiPH_5 \rightarrow \cdot SiH_3^+ + \cdot PH_2$	11.5	265.1	$\Delta H_f^\circ(SiPH_5) = \Delta H_f^\circ(\cdot SiH_3^+) + \Delta H_f^\circ(\cdot PH_2) - ap$	2
			$DE(H_3Si-PH_2) = ap - IP(\cdot SiH_3)$	88
$SiPH_5 \rightarrow \cdot PH_2^+ + \cdot SiH_3$	13.1	302.0	$\Delta H_f^\circ(SiPH_5) = \Delta H_f^\circ(\cdot PH_2^+) + \Delta H_f^\circ(\cdot SiH_3) - ap$	2
			$DE(H_3Si-PH_2) = ap - IP(\cdot PH_2)$	88
			$ea\ (\cdot SiH_3) = -1.5$ ev	-35
			$ea\ (\cdot PH_2) = 0.5$ ev	12

*ΔH_f° = standard enthalpy of formation; DE = dissociation energy; IP = ionization potential; ap = appearance potential; ea = electron affinity; 1 ev = 23.06 kcal/mole; data obtained on the Consolidated Electrodynamics Corp. 21-103c mass spectrometer.

to the right in a row in the periodic table; this assumption is observed since $IP(\cdot PH_2)$ is greater than $IP(\cdot SiH_3)$.

It is gratifying that there is an internal consistency in the values for $\Delta H_f^\circ(SiPH_5)$ and $DE(H_3Si-PH_2)$ despite the two different thermochemical equations employed in the computations. Under the circumstances it is unlikely that this consistency should be altogether fortuitous. Thus, some corroborative support is obtained for the assumption that the appearance-potential values for the fragment ions contain little, if any, excess kinetic energy.

It should be noted that the appearance potentials reported here for silicon-containing fragments were measured on the fragment containing the ^{30}Si isotope. Since this isotope comprises only 3.1% of the silicon isotopes (5), the ions on which the measurements were made were low in abundance, certainly a less favorable experimental situation than if larger ion currents could have been obtained.

Silylgermane (H_3SiGeH_3)

The monoisotopic fragmentation pattern of the positive ions of silylgermane is given in Table 3. These values have been corrected for the isotopic impurities in the silicon and germanium used in the preparation. This pattern agrees well with the fragmentation pattern calculated from the data obtained for silylgermane prepared with silicon and germanium of normal isotopic abundances. Monoisotopic spectra obtained for silane, disilane, germane, and digermane, all prepared using the separated isotopes ^{28}Si and ^{74}Ge, agree with the previously published data (17,18).

Table 3
Fragmentation Pattern of Silylgermane*

Ion	Percent of Total Ion Current	Ion	Percent of Total Ion Current
$GeSiH_6^+$	5.14	GeH_2^+	5.37
$GeSiH_5^+$	2.74	GeH^+	3.56
$GeSiH_4^+$	19.32	Ge^+	6.61
$GeSiH_3^+$	6.03	SiH_3	3.77
$GeSiH_2^+$	15.01	SiH_2	2.59
$GeSiH^+$	9.47	SiH^+	3.88
$GeSi^+$	6.82	Si^+	4.02
GeH_3^+	5.76		

*Data obtained on the CEC 21-103c mass spectrometer.

The appearance potentials of selected ions from the compounds studied and the postulated ion-source processes are presented in Table 4. These values are based on the average of seven measurements for each ion, and the uncertainty cited is the standard deviation. Krypton and argon were used together as internal standards to calibrate the electron-voltage scale and to estimate the absolute accuracy of the measured appearance potentials (±0.2 v).

Supporting data used in these calculations, taken from the work of Gunn and Green (19), are (in kcal/mole): $\Delta H_f^\circ(GeH_4) = 21.6$ and $\Delta H_f^\circ(Si_2H_6) = 37.7$. It has been assumed that the measured appearance potentials given in Table 4 do not contain excess kinetic energy; therefore, the value for $\Delta H_f^\circ(SiGeH_6)$ reported in Table 5 should be taken as a lower limit. The agreement between the values for the heat of formation of silylgermane calculated from the appearance potentials and from postulated processes 6 and 7 of Table 4 is support for the assumption of negligible excess kinetic energy.

Thermochemical values for silylgermane and the silyl and germyl radicals, calculated using equations similar to those described previously, are shown in Table 5. The electron affinities (ea) of $\cdot SiH_3$ and $\cdot GeH_3$ were computed by Neale's method (16). The negative value of the ea for these radicals indicates that they form negative ions nonspontaneously. The excellent agreement with previous results for $\Delta H_f^\circ(\cdot SiH_3^+)$, $\Delta H_f^\circ(\cdot SiH_3)$, $IP(\cdot SiH_3)$, $DE(H_3Si{-}SiH_3)$, and $DE(H_3Si{-}H)$ (22) is gratifying even though it may be fortuitous.

Table 4
Appearance Potentials and Postulated Ion-Source Processes for Silylgermane*

Appearance Potential (ev)	Postulated Process
(1) 10.20 ± 0.03	$GeSiH_6 \rightarrow GeSiH_6^+$
(2) 10.26 ± 0.10	$Ge_2H_6 \rightarrow \cdot GeH_3^+ + \cdot GeH_3$
(3) 10.80 ± 0.07	$GeH_4 \rightarrow \cdot GeH_3^+ + \cdot H$
(4) 11.31 ± 0.12	$Si_2H_6 \rightarrow \cdot SiH_3^+ + \cdot SiH_3$
(5) 11.81 ± 0.09	$SiH_4 \rightarrow \cdot SiH_3^+ + \cdot H$
(6) 11.32 ± 0.14	$GeSiH_6 \rightarrow \cdot GeH_3^+ + \cdot SiH_3$
(7) 12.01 ± 0.09	$GeSiH_6 \rightarrow \cdot SiH_3^+ + GeH_3$

*Data taken on the CEC 21-103c mass spectrometer.

Table 5
Thermochemistry of Silylgermane

Compound	ΔH_f° (Kcal)	DE (Kcal)	IP		EA	
			Kcal	Ev	Kcal	Ev
$\cdot GeH_3^+$	218	–	–	–	–	–
$\cdot GeH_3$	57	–	161	7.0	-32	-1.4
$\cdot SiH_3^+$	227	–	–	–	–	–
$\cdot SiH_3$	50	–	176	7.6	-39	-1.7
$GeSiH_6$	8*	100*	–	–	–	–
$H_3Si-SiH_3$	–	84	–	–	–	–
$H_3Ge-GeH_3$	–	75	–	–	–	–
H_3Si-H	–	95	–	–	–	–
H_3Ge-H	–	87	–	–	–	–
$\cdot GeSiH_3$	–	–	235	10.2	–	–

*Average of the values for processes 6 and 7 cited in Table 2.

However, the use of Franklin's method (23) to calculate $\Delta H_f^\circ(SiGeH_6)$, with pertinent data from Gunn and Green (19) for Si_2H_6 and Ge_2H_6, gives a value of 27.85 kcal/mole, which is approximately 20 kcal/mole more positive than our value but in agreement with the calorimetric measurement of Gunn and Kindsvater (24). The discrepancy between the mass spectrometric value and the calculated and calorimetric values may be explained by the fact that two or more of the radicals or ions involved in the processes shown in Table 4 are energetically nonequivalent due to electronic excitation effects or that the wrong ion-source process was assumed. Unfortunately, it is impossible to check either of these possible errors, although the ionization-efficiency curves do not indicate a complex process occurring in the ion source. It is pointed out that the discrepancy

between the mass spectral and the calculated values can also be explained by the existence of a $(d \rightarrow d)\pi$ interaction. In the case of silylgermane it is difficult to account for the enhanced stability on the basis of differences in electronegativities between the silyl and germyl radicals. However, the lower heat of formation of silylgermane may be rationalized by the existence of $(d \rightarrow d)\pi$ bonds in the compound.

As cited above, the calculated heat of formation is greater than the measured value for $\Delta H_f^\circ(SiGeH_6)$; however, Franklin's computation method (23) was devised primarily for saturated hydrocarbons where $(d \rightarrow d)\pi$ interactions do not occur. The existence of such back-bonding should increase the stability of the molecule if all other bond strengths remain constant; therefore, the measured heat of formation would be expected to be less positive than the calculated value. The existence of back-bonding in silicon compounds has been established by several workers (25,26). Furthermore, Cox's (27) microwave measurements have shown that the Si—Ge bond length in silylgermane is 2.356 ± 0.0005 A; the sum of the covalent radii of silicon and germanium is 2.39 A, indicating definite bond shortening in silylgermane. Thus, the structure and mass spectral data suggest that the 3d electrons of germanium are donated to the vacant 3d orbitals of silicon in silylgermane, forming partial double bonds. This extra bonding could account for the discrepancy between the mass spectral and calculated values for $\Delta H_f^\circ(SiGeH_6)$.

The calorimetric value, although consistent with the intermediate melting and boiling points compared with disilane and digermane, is inconsistent with the measurement of the Si—Ge bond distance. It is difficult to assess the discrepancy between the mass spectral and calorimetric data in view of the past agreement between these two methods for the simple hydrides (17-19). While it is possible that one or more of the ions or radicals involved in Table 4 are energetically nonequivalent due to kinetic energy or electronic excitation effects, the mass spectral data do not indicate any such effects. On the other hand, the assumption relevant to the calorimetric value, that the energy of the solid Sb—Si—Ge mixture produced by the explosion in the calorimeter relative to the separated elements is the same for a mixture of disilane-digermane and silylgermane, may not be entirely valid.

The ionization potential of the germyl radical is lower than that of the silyl radical, agreeing with the concept that the ionization potential should decrease within a chemical group as the atomic number increases. Internal consistency between the values for $\Delta H_f^\circ(SiGeH_6)$ and $DE(H_3SiGeH_3)$, derived from processes 6 and 7 of Table 4, supports the assumption that the measured appearance-potential values do not contain excess kinetic energy; however, there is no absolute assurance of this fact.

Silylarsine (H_3SiAsH_2)

Mass spectral data for silylarsine, arsine, and diarsine are shown in Table 6. No mass spectral properties of the SiH_x^+ (x = 0 . . . 3) fragment ions of silylarsine are reported because tetrasilane, present as an impurity, also serves as a source for these ions.

To calculate the dissociation energy and standard heat of formation for silylarsine from the data given in Table 6, the following ancillary data are required (in kcal/mole): $\Delta H_f^\circ(AsH_3) = 15.9$ (19) and $\Delta H_f^\circ(H_2AsAsH_2) = 35.2$ (18). Although the relative abundances of all of the arsine ions and the appearance potentials for As^+ and AsH^+ agree well with the data previously published (17), the appearance potentials for AsH_2^+ and AsH_3^+ in the two studies are in discord. It has been pointed out by Svec (28) that the appearance potentials for AsH_3^+ and AsH_2^+ cited in the earlier work may have been for an excited state. This seems to be the case, as the value for the ionization potential of AsH_3 reported here agrees well with the value of 10.6 ev cited by Kiser (10).

Table 6
Summary of Mass Spectrometric Results of Silylarsine, Arsine, and Diarsine

Postulated Ion-Source Reaction	Relative Abundance	Ap* (ev)	Ap* (kcal/mole)	Thermochemistry (kcal/mole)
$e^- + H_2As\,^{28}SiH_3 \rightarrow As\,^{28}SiH_5^+ + 2e^-$	59.0	10.1 ± 0.1†	233	$\Delta H_f^\circ(AsSiH_5^+) = ap + \Delta H_f^\circ(H_2AsSiH_3) = 270$
$e^- + H_2As\,^{28}SiH_3 \rightarrow As\,^{28}SiH_4^+ + H + 2e^-$	18.1	11.0 ± 0.3	254	$\Delta H_f^\circ(AsSiH_4^+) = ap + \Delta H_f^\circ(H_2AsSiH_3) - \Delta H_f^\circ(\cdot H) = 239$
$e^- + H_2As\,^{28}SiH_3 \rightarrow As\,^{28}SiH_3^+ + H_2 + 2e^-$	100	9.7 ± 0.1	224	$\Delta H_f^\circ(AsSiH_3^+) = ap + \Delta H_f^\circ(H_2AsSiH_3) - \Delta H_f^\circ(H_2) = 261$
$e^- + H_2As\,^{28}SiH_3 \rightarrow As\,^{28}SiH_2^+ + H_2 + H + 2e^-$	22.5	13.7 ± 0.2	316	$\Delta H_f^\circ(AsSiH_2^+) = ap + \Delta H_f^\circ(H_2AsSiH_3) - \Delta H_f^\circ(H_2) - \Delta H_f^\circ(\cdot H) = 301$
$e^- + H_2As\,^{28}SiH_3 \rightarrow As\,^{28}SiH^+ + 2H_2 + 2e^-$	90.1	13.4 ± 0.1	309	$\Delta H_f^\circ(AsSiH^+) = ap + \Delta H_f^\circ(H_2AsSiH_3) - 2\Delta H_f^\circ(H_2) = 346$
$e^- + H_2As\,^{28}SiH_3 \rightarrow As\,^{28}Si^+ + 2H_2 + H + 2e^-$	41.6	16.8 ± 0.3	387	$\Delta H_f^\circ(AsSi^+) = ap + \Delta H_f^\circ(H_2AsSiH_3) - 2\Delta H_f^\circ(H_2) - \Delta H_f^\circ(\cdot H) = 372$
$e^- + H_2As\,^{28}SiH_3 \rightarrow AsH_3^+ + {}^{28}SiH_2 + 2e^-$	0.1	13.1 ± 0.6	302	$\Delta H_f^\circ(\cdot SiH_2) = ap + \Delta H_f^\circ(H_2AsSiH_3) - \Delta H_f^\circ(AsH_3^+) = 81$
$e^- + H_2As\,^{28}SiH_3 \rightarrow AsH_2^+ + {}^{28}SiH_3 + 2e^-$	42.6	12.4 ± 0.2	286	$\Delta H_f^\circ(H_2AsSiH_3) = \Delta H_f^\circ(AsH_2^+) + \Delta H_f^\circ(\cdot SiH_3) - ap = 37$
				$D(H_2As{-}SiH_3) = ap - IP(\cdot AsH_2) = 73$
$e^- + H_2As\,^{28}SiH_3 \rightarrow AsH^+ + ? + 2e^-$	42.3	...	...	...
$e^- + H_2As\,^{28}SiH_3 \rightarrow As^+ + ? + 2e^-$	56.1	...	...	...
$e^- + AsH_3 \rightarrow AsH_3^+ + 2e^-$	70.2	10.5 ± 0.1	242	$\Delta H_f^\circ(AsH_3^+) = ap + \Delta H_f^\circ(AsH_3) = 258$
$e^- + AsH_3 \rightarrow AsH_2^+ + H + 2e^-$	22.8	13.4 ± 0.2	309	$\Delta H_f^\circ(AsH_2^+) = ap + \Delta H_f^\circ(AsH_3) - \Delta H_f^\circ(\cdot H) = 273$
$e^- + AsH_3 \rightarrow AsH^+ + H_2 + 2e^-$	100	12.5 ± 0.2	288	$\Delta H_f^\circ(AsH^+) = ap + \Delta H_f^\circ(AsH_3) - \Delta H_f^\circ(H_2) = 304$
$e^- + AsH_3 \rightarrow As^+ + H_2 + H + 2e^-$	36.5	15.0 ± 0.3	346	$\Delta H_f^\circ(As^+) = ap + \Delta H_f^\circ(AsH_3) - \Delta H_f^\circ(H_2) - \Delta H_f^\circ(\cdot H) = 310$
$e^- + AsH_3 \rightarrow AsH_3^{2+} + 3e^-$	0.04	...	...	...
$e^- + AsH_3 \rightarrow AsH_2^{2+} + H + 3e^-$	0.3	...	...	...
$e^- + AsH_3 \rightarrow AsH^{2+} + H_2 + 3e^-$	2.2	...	...	...
$e^- + AsH_3 \rightarrow As^{2+} + H_2 + H + 3e^-$	1.5	...	...	...
$e^- + H_2AsAsH_6 \rightarrow AsH_2^+ + AsH_2 + 2e^-$	...	12.9 ± 0.4	298	$\Delta H_f^\circ(\cdot AsH_2) = ap + \Delta H_f^\circ(H_2AsAsH_2) - \Delta H_f^\circ(AsH_2^+) = 60$
				$IP(\cdot AsH_2) = \Delta H_f^\circ(AsH_2^+) - \Delta H_f^\circ(\cdot AsH_2) = 213;$
				$DE(H_2As{-}AsH_2) = ap - IP(\cdot AsH_2) = 85$

*Average of at least seven independent measurements determined by Warren's method of extrapolated differences.
†Standard deviation.
ΔH_f° = standard heat of formation; IP = ionization potential; DE = dissociation energy; 1 ev = 23.06 kcal/mole; data obtained on the Bendix mass spectrometer

Employing the techniques discussed above (therefore, the same errors also apply), the heat of formation and bond energy of silylarsine have been calculated from the appearance-potential data. These values are 37 and 73 kcal/mole, respectively. The heat of formation of the $\cdot SiH_2$ radical, 81 kcal/mole, agrees within experimental error with the value of 72 kcal/mole cited by Vedeneyev, et al. (29). A comparison of the thermal properties of silylarsine and the $\cdot AsH_2$ radical with those reported earlier for silylphosphine and the $\cdot PH_2$ radical shows that $DE(H_2P-SiH_3)$ is more positive than $DE(H_2As-SiH_3)$, agreeing with the concept that the bond energy decreases in a chemical group as the atomic number increases. The data also show that the ionization potential of silylarsine is the same as that of silylphosphine and that the ionization potentials of the radicals $\cdot PH_2$ and $\cdot AsH_2$ are equal. The heats of formation of the ions of arsine, like those of ammonia and phosphine, become more positive with the stepwise removal of hydrogen atoms. Similarly, in the series of ions formed from silylarsine, the loss of one hydrogen atom from the molecular ion yields the ion with the least positive heat of formation, with the heats of formation of the ions becoming more positive with each succeeding loss of hydrogen. The same trend can be noted for the ions produced from the related compound, methylamine.

Phosphorus Trifluoride (PF_3), Phosphorus Oxytrifluoride (POF_3), and Phosphorus Pentafluoride (PF_5)

Mass spectral data for PF_3, POF_3, and PF_5 are shown in Table 7. To calculate the heats of formation of the ions cited in Table 7, the following ancillary values were used (in kcal/mole): $\Delta H_f^\circ(PF_3) = -226.03$ (30), $\Delta H_f^\circ(POF_3) = -286$ (29), $\Delta H_f^\circ(\cdot F) = 18.5$ (31), $\Delta H_f^\circ(P) = 75.3$ (31), $\Delta H_f^\circ(O) = 59.5$ (31), $\Delta H_f^\circ(F^-) = -64.8$ (7), $\Delta H_f^\circ(P^+) = 329$ (7), $\Delta H_f^\circ(F^+) = 420$ (7), $\Delta H_f^\circ(O^-) = 25$ (7), and $\Delta H_f^\circ(PF_5) = -381.4$ (32). It once more has been assumed that the measured appearance potentials contained no excess energies; thus, the limits mentioned previously also apply to the values cited in Table 7. The agreement of the heats of formation found for the various ions common to PF_3 and POF_3 is excellent. The heat of formation of POF_3 (-274.9 kcal/mole) agrees within experimental error with the value of -286 cited by Vedeneyev, et al. (29).

The results for PF_5, on the other hand, indicate some peculiar characteristics. First of all, it should be recalled that the PF_5 results are obtained by difference because the PF_5 could not be separated from POF_3. The results indicate that $\Delta H_f^\circ(PF_3^+)$ from PF_5 is different from the heat of formation of this ion produced from either PF_3 or POF_3. The difference could be explained either by the presence of excitation and/or kinetic energy in the PF_3^+ fragment produced from PF_5 or by the fact that the PF_3^+ formed from PF_5 may be a geometric isomer of the PF_3^+ ion produced from either PF_3 or POF_3. It is impossible to ascertain the reason for the discrepancy from the mass spectral data.

Hydridotrifluorophosphorustricarbonylcobalt [$HCo(CO)_3PF_3$], Hydridobis(trifluorophosphorus)dicarbonylcobalt [$HCo(CO)_2(PF_3)_2$], and Hydridotris(trifluorophosophrus)carbonylcobalt [$HCoCO(PF_3)_3$]

All data reported here were obtained on the modified Bendix T-O-F mass spectrometer. This instrument was used because of its relatively cool ion source, and the fact that the mass spectral data (fragmentation patterns and ionization-efficiency curves) could be obtained very rapidly, thereby reducing the amount of thermal decomposition of the carbonyls in the ion source. In these studies the fragmentation patterns were obtained in less than 2 minutes and the ionization-efficiency curves in less than 1 minute. A fresh sample was admitted into the mass spectrometer for each measurement. Winters and Kiser (33) have reported that frequent ion-source cleaning was necessary in their

Table 7
Mass Spectral Data for PF_3, PF_5, and POF_3

Ion	m/e	Relative Abundance	Ap (ev)	Postulated Process	ΔH°_f (Ion) (kcal/mole)
PF_3^+	88	37.6	11.52 ± 0.12	$PF_3 \rightarrow PF_3^+$	40
PF_2^+	69	100	16.1 ± 0.2	$PF_2^+ + F$	127
PF^+	50	13.4	22.0 ± 0.3	$PF^+ + 2F$	244
P^+	31	8.8	27.9 ± 0.5	$P^+ + 3F$	362
F^+	19	6.6	31.8 ± 0.7	$F^+ + P + F_2$	432
POF_3^+	104	79.4	13.6 ± 0.2	$POF_3 \rightarrow POF_3^+$	39
PF_3^+	88	3.1	16.3 ± 0.5	$PF_3^+ + O$	42
POF_2^+	85	100	14.9 ± 0.2	$POF_2^+ + F$	50
PF_2^+	69	21.2	20.8 ± 0.3	$PF_2^+ + O + F$	(-275)*
POF^+	66	1.1	–	–	–
PF^+	50	10.5	24.6 ± 0.6	$PF^+ + O^- + 2F$	230
PO^+	47	6.9	25.4 ± 0.4	$PO^+ + 3F$	255
P^+	31	7.0	28.3 ± 0.5	$P^+ + O^- + 2F + F^-$	346
F^+	19	2.1	34.6 ± 0.7	$F^+ + P + F + O + F^-$	434
PF_5	126	0	–	–	–
PF_4^+	107	100	16.45 ± 0.1	$PF_5 \rightarrow PF^+ + F$	-20
PF_3^+	88	18.5	21.4 ± 0.2	$PF_3^+ + 2F$	75
PF_2^+	69	6.0	22.1 ± 0.3	$PF_2^+ + 2F + F^-$	156
PF^+	50	9.5	27.8 ± 0.5	$PF^+ + F_2 + 2F$	228
P^+	31	2.0	32.0 ± 0.8	$P^+ + 4F + F^-$	347
F^+	19	3.2	–	–	–

*Heat of formation of POF_3. Data obtained on the Bendix mass spectrometer

study of dicobalt octacarbonyl. The same situation was true for the compounds investigated in this study, and the ion source, electron multiplier, and Philips gauge were cleaned after every 4 hours of operation.

Mass spectral fragmentation patterns for the three cobalt carbonyl hydrides are shown in Table 8. In addition to the ions reported, a number of ions of minor abundance (<3%) were also observed. These included ion species which result from the loss of an oxygen atom from one of the carbon monoxide ligands or a fluorine atom from one of the phosphorus trifluoride moieties. All of the compounds give rise to moderately intense parent ion currents, but none of the parent ions loses a hydrogen atom. Further, when considering the pairs of ion currents separated by one mass unit throughout each of the spectra, the hydrogen-containing ions are more abundant than the ions which have lost a hydrogen atom until two or more species either CO or PF_3) are fragmented from the parent ion. This type of fragmentation trend has been observed in $HCo(CO)_4$ (34) and $HMn(CO)_5$ (35) and can be explained by an interaction between the equitorial ligands (either CO or PF_3) and the axial H atom. No doubly charged ions were observed in the spectra above m/e = 50.

Table 8
Fragmentation Patterns of $HCo(CO)_x(PF_3)_{4-x}$*

m/e	Ion Species	$HCo(CO)_3PF_3$	$HCo(CO)_2(PF_3)_2$	$HCoCO(PF_3)_3$
352	$HCo(CO)(PF_3)_3^+$	–	–	7.8
324	$HCo(PF_3)_3^+$	–	–	2.6
292	$HCo(CO)_2(PF_3)_2^+$	–	14.3	–
264	$HCo(CO)(PF_3)_2^+$	–	15.7	13.4
263	$Co(CO)(PF_3)_2^+$	–	1.0	4.2
236	$HCo(PF_3)_2^+$	–	0.8	5.9
235	$Co(PF_3)_2^+$	–	1.2	7.6
232	$HCo(CO)_3(PF_3)^+$	9.2	–	–
204	$HCo(CO)_2(PF_3)^+$	17.8	16.1	–
203	$Co(CO)_2(PF_3)^+$	2.3	5.1	–
176	$HCo(CO)(PF_3)^+$	7.7	16.9	17.2
175	$Co(CO)(PF_3)^+$	17.3	34.4	34.4
148	$HCo(PF_3)^+$	4.4	8.6	13.9
147	$Co(PF_3)^+$	18.7	39.6	63.0
144	$HCo(CO)_3^+$	4.1	–	–
143	$Co\ (CO)_3^+$	4.9	–	–
116	$HCo(CO)_2^+$	13.6	9.4	1.1
115	$Co(CO)_2^+$	47.8	31.9	4.6
88	$HCo(CO)^+$	19.5	17.9	18.2
87	$Co(CO)^+$	78.2	72.3	48.2
69	PF_2^+	10.0	19.2	32.0
60	HCo	7.5	8.4	9.8
59	Co^+	100	100	100
28	CO^+	56.0	32.1	27.2

*Ionizing current = 0.125 μamp; Bendix T-O-F instrument in pulsed mode with the ion; 70 v.

Although an attempt was made to study the negative ions produced from these cobalt carbonyl hydrides, these ions were few in number and very low in intensity. It appeared that the negative ions were formed primarily from an electron-capture process since their intensity was maximized at an electron energy in the range of 2 to 6 v. However, due to instrumental limitations, the data obtained for negative ions are not definitive.

Clastograms (a plot of the relative ion abundance versus electron energy) showed that the unimolecular decomposition of these cobalt carbonyl hydrides occurred in a series of successive eliminations of either carbon monoxide or phosphorus trifluoride, similar to the decomposition of dicobalt octacarbonyl observed by Winters and Kiser (33). To calculate the heats of formation of either the compounds or positive ions investigated in this study, the following ancillary data were required (in kcal/mole): $\Delta H_f^\circ(\cdot H) = 52.1$ (31), $\Delta H_f^\circ(Co^+) = 287.3$ (36), $\Delta H_f^\circ(CO) = -26.4$ (36), $\Delta H_f^\circ(PF_3) = -226.0$ (30), $\Delta H_f^\circ(Co(CO)_3^+) = 70$ (33), $\Delta H_f^\circ(Co(CO)_3^+) = 138$ (33), $\Delta H_f^\circ(Co(CO)^+) = 203$ (33). The ions, appearance potentials, and assumed neutral products for the three compounds are tabulated in Tables 9, 10, and 11. It has again been assumed that the measured appearance potentials do not contain excess kinetic or excitation energy. The rather large error limits are probably due to the speed with which the data were taken, thereby emphasizing the statistical fluctuations in the ion currents.

Table 9
Appearance-Potential Data for $HCo(CO)_3PF_3$

Ion	Neutral Products	Appearance Potential*	
		Ev	Kcal
$HCo(CO)_3(PF_3)^+$	–	9.8 ± 0.2†	226.0
$HCo(CO)_2(PF_3)^+$	CO	10.3 ± 0.3	237.5
$HCo(CO)(PF_3)^+$	2CO	12.5 ± 0.3	288.2
$Co(CO)(PF_3)^+$	2CO + H	14.3 ± 0.3	329.8
$HCo(PF_3)^+$	3CO	13.8 ± 0.2	318.2
$Co(PF_3)^+$	3CO + H	15.7 ± 0.4	362.0
$HCo(CO)_3^+$	PF_3	9.9 ± 0.2	228.3
$Co(CO)_3^+$	PF_3 + H	12.1 ± 0.4	279.0
$HCo(CO)_2^+$	Co + PF_3	12.4 ± 0.3	286.0
$Co(CO)_2$	CO + PF_3 + H	14.0 ± 0.4	322.8
$HCo(CO)^+$	2CO + PF_3	12.1 ± 0.2	279.0
$Co(CO)^+$	2CO + PF_3 + H	15.5 ± 0.4	357.4
HCo^+	3CO + PF_3	14.6 ± 0.5	336.7
Co^+	3CO + PF_3 + H	17.8 ± 0.6	410.5

*Average of at least seven independent measurements determined by Warren's method of extrapolated differences: Calibrating gas was Ar; IP = 15.755 v.
†Standard deviation.

Table 10
Appearance-Potential Data for $HCo(CO)_2(PF_3)_2$

Ion	Neutral Products	Appearance Potential*	
		Ev	Kcal
$HCo(CO)_2(PF_3)_2^+$	–	9.6 ± 0.2†	221.4
$HCo(CO)(PF_3)_2^+$	CO	10.3 ± 0.3	237.5
$HCo(CO)_2(PF_3)^+$	PF_3	10.1 ± 0.2	232.9
$HCo(CO)(PF_3)^+$	$CO + PF_3$	12.4 ± 0.4	286.0
$Co(CO)(PF_3)^+$	$CO + +F_3 + H$	14.0 ± 0.3	322.8
$HCo(PF_3)^+$	$2CO + PF_3$	13.6 ± 0.3	313.6
$Co(PF_3)^+$	$2CO + PF_3 + H$	15.9 ± 0.4	366.7
$HCo(CO)_2^+$	$2PF_3$	11.6 ± 0.2	267.5
$Co(CO)_2^+$	$2PF_3 + H$	13.6 ± 0.4	313.6
$HCo(CO)^+$	$CO + 2PF_3$	12.3 ± 0.2	283.6
$Co(CO)^+$	$CO + 2PF_3 + H$	15.3 ± 0.5	352.8
HCo^+	$2CO + 2PF_3$	14.9 ± 0.7	343.6
Co^+	$2CO + 2PF_3 + H$	18.2 ± 0.5	419.7

*Average of at least seven independent measurements determined by Warren's method of extrapolated differences: Calibrating gas was Ar; IP = 15.755 v.
†Standard deviation.

The thermochemical results are summarized in Table 12. The values of the heats of formation for $HCo(CO)_3PF_3$, $HCo(CO)_2(PF_3)_2$, and $HCoCO(PF_3)_3$ are (in kcal/mole) -381, -579, and -783, respectively. It is seen that the heat of formation of the compounds becomes approximately 200 kcal/mole more negative as phosphorus trifluoride is substituted for carbon monoxide. Since this variation is very nearly the difference between the heats of formation of phosphorus trifluoride and carbon monoxide, the nature of the cobalt-carbon and the cobalt-phosphorus bonds must be quite similar. The calculated heats of formation of $HCo(CO)_3PF_3$ from different assumed ion-source processes are in agreement with each other. This internal agreement supports Winters and Kiser's value (33) of -132 kcal/mole for $\Delta H_f^\circ(\cdot Co(CO)_4)$. The heat of formation of $HCo(CO)_3PF_3$ calculated using the Co^+ is independent of Winters and Kiser's estimate of the heat of formation of the cobalt tetracarbonyl radical, while the heats of formation calculated from the other ion-source processes are based on the estimated heat of formation of the radical. The same observation is noted for the data obtained from $HCo(CO)_2(PF_3)_2$ and $HCoCO(PF_3)_3$.

Table 11
Appearance-Potential Data for $HCoCO(PF_3)_3$

Ion	Neutral Products	Appearance Potential*	
		Ev	Kcal
$HCo(CO)(PF_3)_3^+$	–	10.2 ± 0.1†	235.2
$HCo(PF_3)_3^+$	CO	11.1 ± 0.2	256.0
$HCo(CO)(PF_3)_2^+$	PF_3	10.4 ± 0.3	239.8
$HCo(PF_3)_2^+$	Co + PF_3	12.6 ± 0.2	290.6
$Co(PF_3)_2^+$	CO + PF_3 + H	14.5 ± 0.4	334.4
$HCo(CO)(PF_3)^+$	$2PF_3$	12.3 ± 0.3	283.6
$Co(CO)(PF_3)^+$	$2PF_3$ + H	14.1 ± 0.3	325.2
$HCo(PF_3)^+$	CO + $2PF_3$	13.6 ± 0.2	313.6
$Co(PF_3)^+$	CO + $2PF_3$ + H	15.7 ± 0.5	362.0
$HCo(CO)^+$	$3PF_3$	12.0 ± 0.2	276.7
$Co(CO)^+$	$3PF_3$ + H	15.9 ± 0.4	366.7
HCo^+	CO + $3PF_3$	15.6 ± 0.3	359.8
Co^+	CO + $3PF_3$ + H	17.8 ± 0.6	410.5

*Average of at least seven independent measurements determined by Warren's method of extrapolated differences: Calibrating gas was Ar; IP = 15.755 v.
†Standard deviation.

CONCLUSIONS

These studies have demonstrated that a mass spectrometer can be used to determine such important thermodynamic properties as bond energies and heats of formation of unstable inorganic materials. Where literature values were available, there was usually good agreement between the thermochemical values determined by mass spectrometric measurement and those found by other methods. However, the mass spectrometer can use a much smaller amount of sample for the thermochemical measurement than any of the other more commonly used methods of thermochemical data acquisition. Although there are several possible sources of error in a mass spectrometric thermochemical determination, it is often the only method by which these important properties can be determined for many of the transient and highly reactive molecules and radicals.

ACKNOWLEDGMENTS

It is indeed a pleasure to acknowledge the aid of many people involved in the studies reported here. Professor H. J. Svec of Iowa State University collaborated with the authors on the silylphosphine and silylgermane phases of the work; Professor R. W. Kiser of the University of Kentucky and Kansas State University cooperated in the work reported

Table 12
Heats of Formation in Kcal/Mole of the Positive Ions
Produced from $HCo(CO)_x(PF_3)_{4-x}$

Ion	Compound		
	$HCo(CO)_3PF_3$	$HCo(CO)_2(PF_3)_2$	$HCoCO(PF_3)_3$
$HCo(CO)(PF_3)_3^+$	–	–	-547
$HCo(PF_3)_3^+$	–	–	-500
$HCo(CO)_2(PF_3)_2^+$	–	-357	–
$HCo(CO)(PF_3)_2^+$	–	-316	-317
$Co(CO)(PF_3)_2^+$	–	–	–
$HCo(PF_3)_2^+$	–	–	-240
$Co(PF_3)_2^+$	–	–	-248
$HCo(CO)_3(PF_3)^+$	-155	–	–
$HCo(CO)_2(PF_3)^+$	-117	-120	–
$Co(CO)_2(PF_3)^+$	–	–	–
$HCo(CO)(PF_3)^+$	-40	-40	-47
$Co(CO)(PF_3)^+$	-51	-56	-58
$HCo(PF_3)^+$	16	14	9
$Co(PF_3)^+$	8	14	6
$HCo(CO)_3^+$	74	–	–
$Co(CO)_3^+$	70* (-383)†	70* ...	70* ...
$HCo(CO)_2^+$	157	141	–
$Co(CO)_2^+$	138* (-385)†	138* (-576)†	138* ...
$HCo(CO)^+$	177	183	172
$Co(CO)^+$	203* (-381)†	203* (-576)†	203* (-790)†
HCo^+	261	270	282
Co^+	287* (-376)†	287* (-589)†	287* (-776)†
Avg. $\Delta H_f^\circ[HCo(CO)_x(PF_3)_{4-x}]$	(-381)†	(-579)†	(-783)†

*Literature value; Refs. 33 and 36.
†Number in parentheses are heats of formation of the compounds calculated using the literature value of the heat of formation of the appropriate ion. Final value in the heat of formation column is the numerical average of the heats of formation calculated from the various ions.

for PF_3, PF_5, and POF_3; finally, Professor A. G. MacDiarmid and Dr. Surinder K. Gondal of the University of Pennsylvania furnished the compounds used in the cobalt hydride portion of this report. To all of these gentlemen we extend our gratitude.

REFERENCES

1. Kagarise, R.E., and Saunders, R.A., "The Analysis of Contaminants in Aviators' Breathing Oxygen," NRL Report 5554, Oct. 1960

2. Saunders, R.A., and Saalfeld, F.E., "Improved Methods of the Detailed Analysis of Trace Contaminants in Submarine Atmospheres," Chapter 5 in "Fourth Annual Progress Report on the Present Status of Chemical Research in Atmosphere Purification and Control on Nuclear-Powered Submarines," Lockhart, L.B., Jr., and Piatt, V.R., editors, NRL Report 6251, Mar. 1965

3. Saalfeld, F.E., and McDowell, M.V., "A Mass Spectrometric Method for the Determination of Permeability Coefficients," NRL Report 6182, Dec. 1964

4. Saalfeld, F.E., and McDowell, M.V., "Diffusion Rates of Methyl Chloroform Through Some Insulation Materials," NRL Report 6302, July 1965

5. Beynon, J.H., "Mass Spectrometry and its Applications to Organic Chemistry," New York:Elsevier, Chapter 1, 1960

6. Waldron, J.D., and Wood, K., "Mass Spectrometry," London:Institute of Petroleum, p. 16, 1952

7. Field, F.H., and Franklin, J.L., "Electron Impact Phenomena and the Properties of Gaseous Ions," New York:Academic Press, 1957

8. Flesch, G.D., and Svec, H.J., J. Am. Chem. Soc. 81:1787 (1959)

9. Kiser, R.W., and Gallegos, E.J., J. Phys. Chem. 66:947 (1962)

10. Kiser, R.W., "Introduction to Mass Spectrometry and its Applications," Englewood Cliffs, New Jersey:Prentice-Hall, 1965

11. Olfky, R.S., and Saalfeld, F.E., "An Apparatus for Simultaneously Measuring Multiple Threshold Potentials with a Time-of-Flight Mass Spectrometer," Rept. of NRL Prog., p. 56, June 1965

12. Drake, J.E., and Jolly, W.L., Chem. Ind. (London) 1470 (1962)

13. Sanderson, R.T., "Vacuum Manipulation of Volatile Compounds," New York:Wiley, 1948

14. Spanier, E.J., and MacDiarmid, A.G., Inorg. Chem. 2:215 (1963)

15. Piper, T.S., and Wilson, M.K., J. Inorg. Nucl. Chem. 4:22 (1957)

16. Neale, R.S., J. Phys. Chem. 68:143 (1964)

17. Saalfeld, F.E., and Svec, H.J., Inorg. Chem. 2:46 (1963)

18. Saalfeld, F.E., and Svec, H.J., Inorg. Chem. 2:50 (1963)

19. Gunn, S.R., and Green, L.G., J. Phys. Chem. 65:779 (1961)

20. Steele, W.C., Nichols, L.D., and Stone, F.G.A., J. Am. Chem. Soc. 84:4441 (1962)

21. Wada, Y., and Kiser, R.W., Inorg. Chem. 3:174 (1964)

22. Saalfeld, F.E., and Svec, H.J., Inorg. Chem. 3:1442 (1964)

23. Franklin, J.L., Ind. Eng. Chem. 41:1070 (1949)

24. Gunn, S.R., and Kindsvater, J.H., J. Phys. Chem. 70:1750 (1966)

25. Davidson, G., Ebsworth, E.A., Sheldrick, G.M., and Woodward, C.A., Chem. Comm. (London) No. 7, 122 (1965)

26. Goodman, L., Konstam, A.H., and Sommer, L.H., J. Am. Chem. Soc. 87:1012 (1965)

27. Cox, A.P., private communication of unpublished results, 1965

28. Svec, H.J., "Mass Spectrometry," Reed, R.I., editor, New York:Academic Press, p. 245, 1966

29. Vedeneyev, V.I., Gurvich, L.V., Kondrat'yev, V.N., Medvedev, V.A., and Frankevich, Ye.L., "Bond Energies, Ionization Potentials, and Electron Affinities," London: Edward Arnold Publishers, p. 135, 1966

30. Duus, H.C., and Mykytiuk, D.P., J. Chem. Eng. Data 9:585 (1964)

31. Cottrell, T.L., "The Strengths of Chemical Bonds," 2nd ed., London:Butterworth, 1958

32. Gross, P., Hayman, C., and Stuart, M.C., Trans. Faraday Soc. 62:2716 (1966)

33. Winters, R.E., and Kiser, R.W., J. Phys. Chem. 69:1618 (1965)

34. Saalfeld, F.E., unpublished data

35. Edgell, W.F., and Risen, W.M., Jr., J. Am. Chem. Soc. 88:5451 (1966)

36. Rossini, F.D., Wagman, D.D., Evans, W.H., Levine, S., and Jaffe, I., "Selected Values of Chemical Thermodynamic Properties," National Bureau of Standards Cir. 500, Superintendent of Documents, U.S. Government Printing Office, Washington, D.C., 1952

This page intentionally left blank.

Security Classification

DOCUMENT CONTROL DATA - R & D

(Security classification of title, body of abstract and indexing annotation must be entered when the overall report is classified)

1. ORIGINATING ACTIVITY *(Corporate author)* Naval Research Laboratory Washington, D.C. 20390	2a. REPORT SECURITY CLASSIFICATION Unclassified 2b. GROUP

3. REPORT TITLE

ELECTRON IMPACT STUDIES OF VOLATILE INORGANIC COMPOUNDS

4. DESCRIPTIVE NOTES *(Type of report and inclusive dates)*

This is an interim report; work is continuing on all phases of the problem.

5. AUTHOR(S) *(First name, middle initial, last name)*

F.E. Saalfeld and M.V. McDowell

6. REPORT DATE November 22, 1967	7a. TOTAL NO. OF PAGES 30	7b. NO. OF REFS 36
8a. CONTRACT OR GRANT NO. NRL Problem C07-02 b. PROJECT NO. RR 001-01-43-4804 c. d.	9a. ORIGINATOR'S REPORT NUMBER(S) NRL Report 6639 9b. OTHER REPORT NO(S) *(Any other numbers that may be assigned this report)*	

10. DISTRIBUTION STATEMENT

This document has been approved for public release and sale; its distribution is unlimited.

11. SUPPLEMENTARY NOTES	12. SPONSORING MILITARY ACTIVITY Department of the Navy (Office of Naval Research) Washington, D.C. 20360

13. ABSTRACT

The appearance potential of an ion is defined as the minimum energy of bombarding electrons required to produce that ion from a particular atom or molecule. This potential can be estimated from ionization-efficiency curves by various methods, such as the initial break method, linear extrapolation method, critical slope method, extrapolated difference method, second derivative method, ratio extrapolation method, and energy compensation method.

By the use of appearance-potential data obtained from the mass spectrometer, the bond energies and heats of formation of unstable inorganic materials can be determined. Although there are several possible sources of error in a mass spectrometric thermochemical determination, it is often the only method by which these important properties can be determined for many of the transient and highly reactive molecules and radicals.

Where literature values were available, there was usually good agreement between the thermochemical values determined by mass spectrometric measurement and those found by other methods.

DD FORM 1 NOV 65 1473 (PAGE 1)

S/N 0101-807-6801

Security Classification

Security Classification

14 KEY WORDS	LINK A ROLE	LINK A WT	LINK B ROLE	LINK B WT	LINK C ROLE	LINK C WT
Mass spectrometer						
Appearance potential						
Ionization efficiency						
Mass-to-charge ratios						
Dissociation energy						
Ionization potential						
Ion-source reaction						
Fragmentation pattern						
Silylphosphine						
Silylgermane						
Silylarsine						
Phosphorus trifluoride						
Phosphorus oxytrifluoride						
Phosphorus pentafluoride						
Hydridotrifluorophosphorustricarbonylcobalt						
Hydridobis(trifluorophosphorus)dicarbonylcobalt						
Hydridotris(trifluorophosphorus)carbonylcobalt						

DD FORM 1 NOV 65 1473 (BACK) (PAGE 2)

GPO 934-243

Security Classification